Optical Engineering

SPIEDigitalLibrary.org/oe

Image stitching and image reconstruction of intestines captured using radial imaging capsule endoscope

Mang Ou-Yang
Wei-De Jeng
Yin-Yi Wu
Lan-Rong Dung
Hsien-Ming Wu
Ping-Kuo Weng
Ker-Jer Huang
Luan-Jiau Chiu

Image stitching and image reconstruction of intestines captured using radial imaging capsule endoscope

Mang Ou-Yang
National Chiao-Tung University
Department of Electrical Engineering
Hsinchu City 30010, Taiwan

Wei-De Jeng
Yin-Yi Wu
National Chiao-Tung University
Department of Electrical and Control Engineering
Hsinchu City 30010, Taiwan
E-mail: jwd.ece99g@nctu.edu.tw

Lan-Rong Dung
National Chiao-Tung University
Department of Electrical Engineering
Hsinchu City 30010, Taiwan

Hsien-Ming Wu
Ping-Kuo Weng
Ker-Jer Huang
Luan-Jiau Chiu
Chung-Shan Institute of Science and Technology
Lung-Tan 90008-8-8, Taiwan

Abstract. This study investigates image processing using the radial imaging capsule endoscope (RICE) system. First, an experimental environment is established in which a simulated object has a shape that is similar to a cylinder, such that a triaxial platform can be used to push the RICE into the sample and capture radial images. Then four algorithms (mean absolute error, mean square error, Pearson correlation coefficient, and deformation processing) are used to stitch the images together. The Pearson correlation coefficient method is the most effective algorithm because it yields the highest peak signal-to-noise ratio, higher than 80.69 compared to the original image. Furthermore, a living animal experiment is carried out. Finally, the Pearson correlation coefficient method and vector deformation processing are used to stitch the images that were captured in the living animal experiment. This method is very attractive because unlike the other methods, in which two lenses are required to reconstruct the geometrical image, RICE uses only one lens and one mirror. [DOI: 10.1117/1.OE.51.5.057004]

Subject terms: radial imaging capsule endoscope; mean absolute error; mean square error; pearson correlation coefficient; peak signal-to-noise ratio; stitch images; correlation.

Paper 111503 received Dec. 1, 2011; revised manuscript received Feb. 29, 2012; accepted for publication Mar. 1, 2012; published online May 4, 2012.

1 Introduction

Diseases of the intestine are very difficult to treat because the intestine is very long and winding. Although the colonoscopy has been available for many years, it is still very difficult to use to obtain internal images because the length of intestine is about 7 m. Therefore, the Given Image Co. (Yoqneam, Israel) proposed a first-generation capsule endoscope called the M2A capsule endoscope.[1,2] After this new endoscope entered the market, several companies and laboratories began conducting relevant research. They included a radio frequency (RF) system laboratory, Olympus in Japan,[3] and Intelligent Microsystems in Korea, China, and Taiwan.[4,5] The capsule endoscope, developed several years ago, solved the main problems of capturing images inside the intestine.[6] Unfortunately, this kind of capsule endoscope can take only the front images; therefore, it also is known as front imaging capsule endoscope (FICE).[7] However, about 50,000 images are captured during a typical period of treatment, and having a doctor examine these images one at a time takes a long time. Therefore, this work develops a new generation of radial imaging capsule endoscopes (RICE) with a different imaging method, in which a cone mirror is used to obtain radial images.[7] In the RICE system, the regions in the images that are captured at different times have overlap, as shown in Fig. 1. The image from the interior toward the exterior, black, green, white, and blue in concentric rings when t is zero. Then, RICE moves forward to $t = 1$; the image then becomes green, white, and blue in concentric rings from the interior toward the exterior; similarly at t is 2 and 3. From this example, RICE provides images that can be related to each other, enabling the complete image to be reconstructed.[7] The images can be combined using a mathematical algorithm, enabling doctors to diagnose a disease more effectively because they do not need to examine these images one at a time.

However, some problems are encountered with the RICE system. They fall into two categories: imaging and lighting. With respect to the former, the cone mirror increases aberration and compresses the image, reducing the image resolution.[7] The structure of the RICE system differs from that of the FICE system. In the FICE system, the problem of stray light is solved by putting the LEDs on the elliptical focal plane of the dome, because of the stationarity optical path length.[8] However, the RICE system is composed of an extra cone mirror, so the problems of stray light and overblooming are very serious. Accordingly, this work mainly focuses on stitching the sequential images using different algorithms and solving the lighting and imaging problems by image processing. Finally, the image is reconstructed after image stitching.

2 Radial Imaging

2.1 *RICE Component*

The greatest difference between RICE and FICE is in the imaging: the RICE system uses a cone mirror, but the other components, such as the imager, illuminator, viewing window, and optical module, do not differ much from those

0091-3286/2012/$25.00 © 2012 SPIE

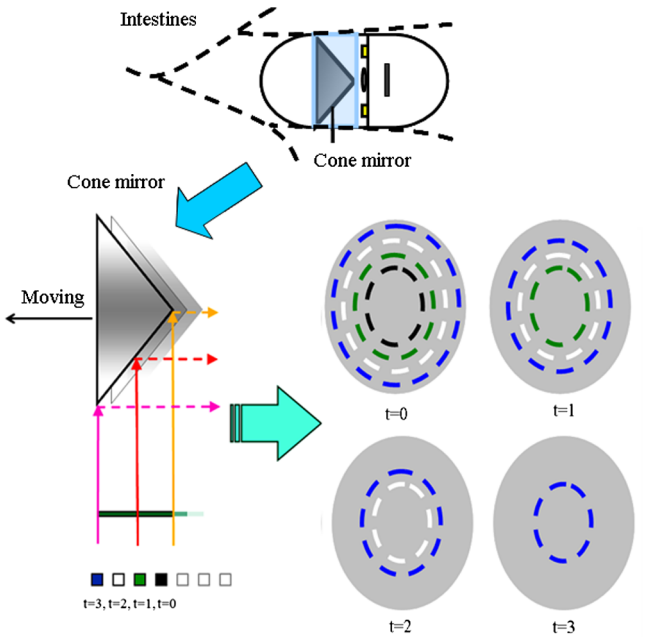

Fig. 1 The images have overlapping regions in the RICE system.

in the FICE system.[7] Table 1 compares RICE with FICE; RICE uses a cone mirror and lenses to capture radial images, and the CCD resolution and pixel size are the same compared to FICE.

2.2 *Radial Imaging Processing*

This section introduces image processing in the RICE system. Figure 2 shows the steps. First, the RICE passes through a cylindrical object and takes photographs at different times. Second, the images are "unwrapped" by performing a coordinate transformation. Finally, an algorithm is utilized to stitch the unwrapped images and construct geometrical image of the object.

Table 1 The configuration comparison between FICE and RICE.

	Capsule	
Item	FICE	RICE
CCD resolution	512 × 512	512 × 512
Pixel size	5.6 μm	5.6 μm
LED	White × 6	White × 6
Imaging region	Front region	Side region (radial imaging)
Window type	Semispherical type	Annular type
Imaging component	Doublet lens	Doublet lens and cone mirror
Cone mirror size	None	3.35 mm

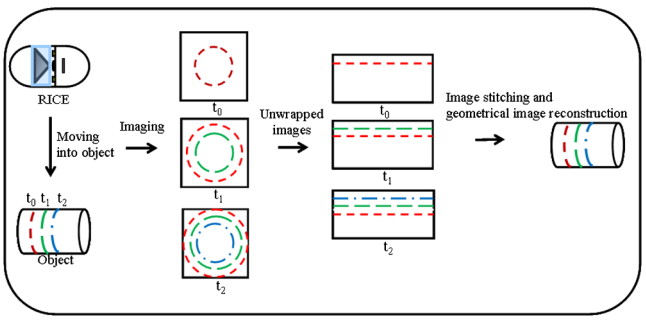

Fig. 2 The image-processing steps of the RICE system.

3 Analysis of RICE Imaging Properties

3.1 *Compression of Images*

The geometry of the cone mirror causes the problem of image compression in the RICE system. Each image is severely compressed when close to its center. This effect is also called warping, and it is shown in Fig. 3. Clearly, images obtained using the RICE system can be treated as having polar coordinates. They are unwrapped by a coordinate transformation, using equations such as Eqs. (1) and (2).[9] In Fig. 3, $f(x, y)$ represents a warped image; $O(x_0, y_0)$ is

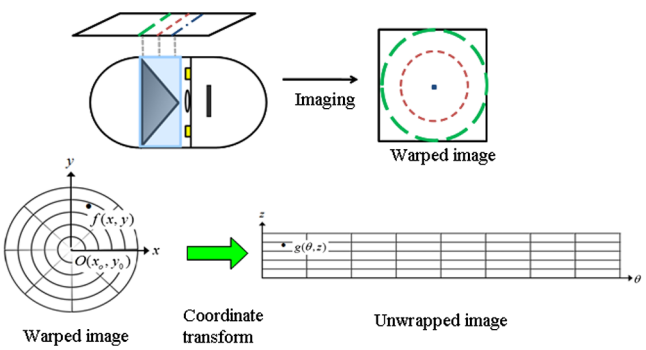

Fig. 3 The top part reveals that the images are compressed by cone mirror; the bottom part shows the image is unwrapped by coordinate transform.

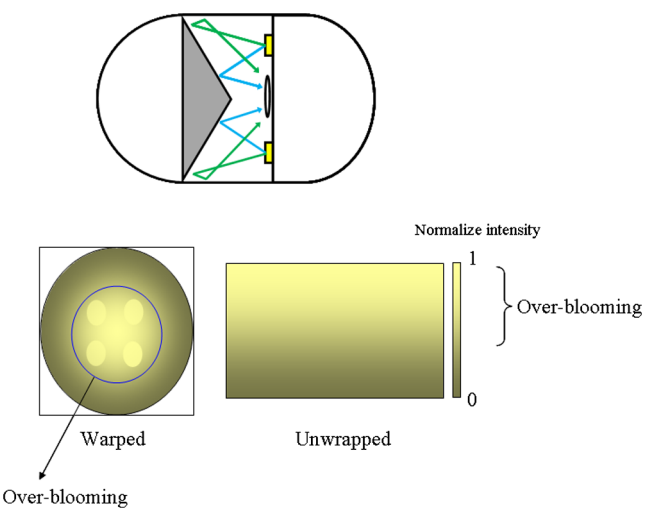

Fig. 4 A lighting problem in RICE causes over-blooming and low lighting uniformity.

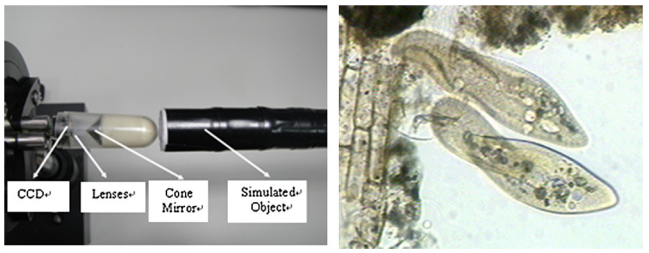

Fig. 5 (a) The experimental apparatus of RICE and (b) a simulated object sample.

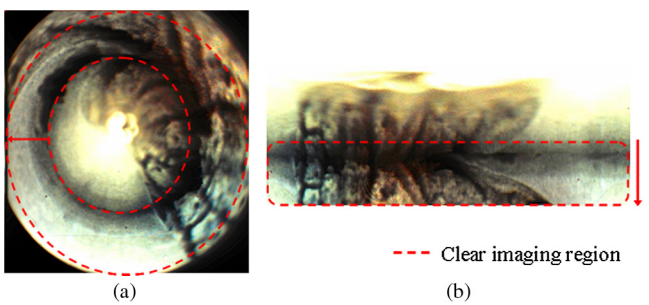

Fig. 6 (a) The clear imaging region of warped and (b) unwrapped images.

the center of the warped image, and $g(\theta, z)$ is the unwrapped image obtained by applying Eqs. (1) and (2) to the warped image.

$$z = \sqrt{(x - x_0)^2 - (y - y_0)^2} \tag{1}$$

$$\theta = \tan^{-1}\left(\frac{y - y_0}{x - x_0}\right). \tag{2}$$

3.2 *Stray Light Problem in RICE System*

A good optical system must include effective lighting and imaging. Lighting can seriously affect image quality in the RICE system. An object can be illuminated with LEDs, but such a setup produces stray light and over-blooming. The light emitting from LEDs scatters on the annular transparent viewing window or reflects on the cone mirror, and then these rays pass through lenses without carrying any information about the object, as shown in Fig. 4.[10] The over-blooming part will move to the top of the image when it is unwrapped.

3.3 *Image Stitching Algorithms*

Image stitching has been developed over a long period of time. It is always used in panoramic systems, which take a sequence of mutually related photographs at different times. RICE can also be applied as a panoramic system, which requires image stitching. The correlation between two sets of data can be computed mathematically using several methods. These include feature-based robust estimation,[11] the multi-resolution method,[12] scale-invariant feature transformation (SIFT),[13] statistical methods, and energy maps.[14] In this study, three statistical algorithms are used to stitch images in the RICE system. These are the mean absolute error (MAE), mean square error (MSE) and Pearson correlation coefficient-based methods. The corresponding formulas are Eqs. (3) through (5), respectively. The MAE uses an error to describe the difference between two sets of data. If the value is low, then the sets of data are highly correlated. The MSE method is based on the same concept, but the value depends on the square of the difference between data.[15–18] The Pearson correlation coefficient $C(x, y)$ is a statistic that is obtained by computing the covariance and variance of data sets, a value of close to unity means a strong correlation.[19,20]

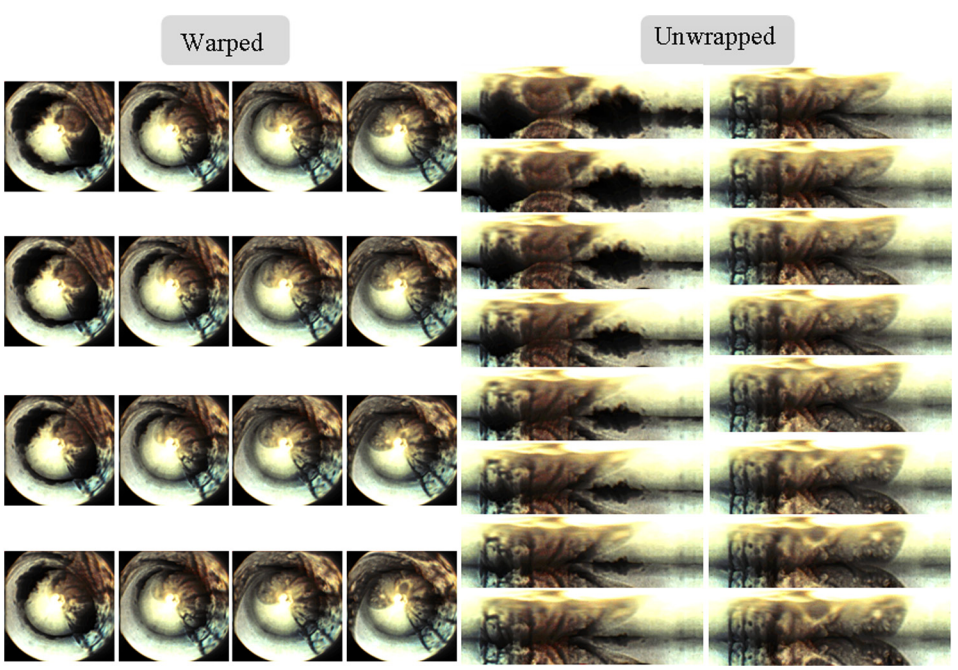

Fig. 7 The warped images (captured by RICE) and unwrapped images.

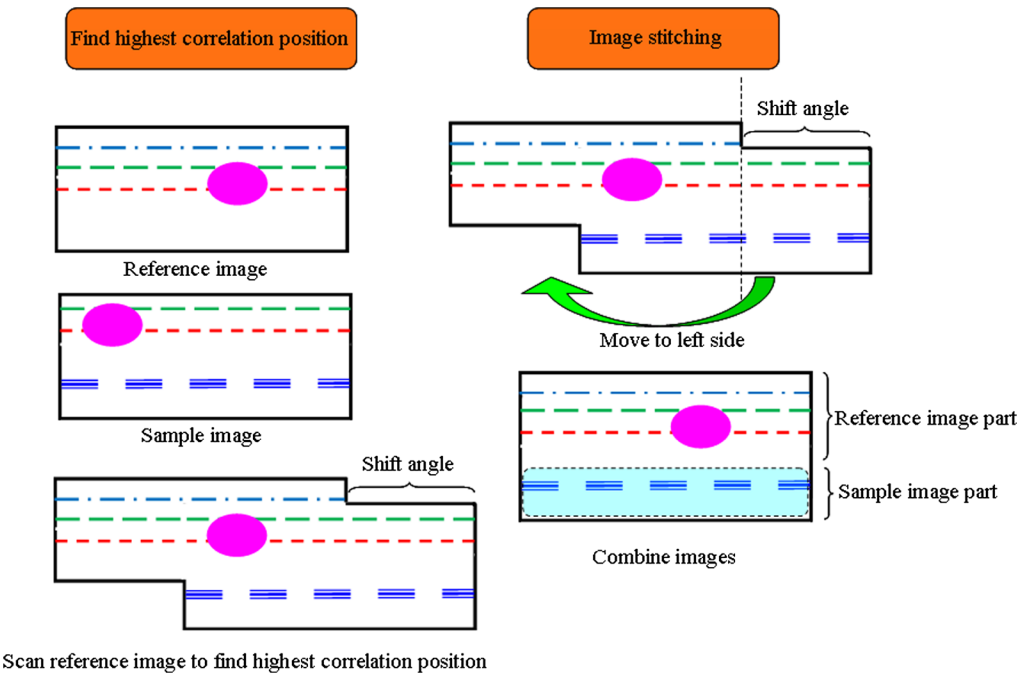

Fig. 8 The steps of image stitching.

$$\mathrm{MAE} = \frac{1}{m \times n} \sum_{i=0}^{m \times n - 1} |S(i) - R(i)| \tag{3}$$

$$\mathrm{MSE} = \frac{1}{m \times n} \sum_{i=0}^{m \times n - 1} |S(i) - R(i)|^2 \tag{4}$$

$$C(x,y) = \frac{\sum_m \sum_n [S(m,n) - u_s][R(m-x,n-y) - u_R]}{\sqrt{\sum_m \sum_n [S(m,n) - u_s]^2} \sqrt{\sum_m \sum_n [R(m-x,n-y) - u_R]^2}}. \tag{5}$$

S is a sample image; R is the reference image; $m \times n$ is image size; x and y are the points of the highest correlation between S and R computed from the Pearson correlation coefficient, and μ_S and μ_R are the average of the sample and reference images. Hence, when the highest position of the highest correlation between the sample and reference images is determined, the images can be stitched by shifting the sample image to this position and the reference and sample images then combined.

4 Experiments and Image Processing

4.1 *Experimental Setup and Image Capture*

An experiment is carried out using RICE to capture radial images. The object is a tube, to mimic an intestine. The left side of Fig. 5 shows the experimental devices, including the CCD, lenses, the cone mirror, and a simulated object. The simulated object is a paramecium figure, which shown on the right side of Fig. 5.[7] A paramecium figure is chosen because it has a complex shape with many edges, and so can be used to test whether the image-stitching algorithm is strong. A triaxial platform is utilized to move the RICE, and the shot rate is one image per millimeter. The RICE scanning of the object yields 70 images, which can be processed using the above algorithm.

Before the images can be stitched, they must be unwrapped using Eqs. (1) and (2). The $O(x_0, y_0)$ of the warped image is (241, 241) because this point corresponds to the optical axis in the image plane. Figure 6 shows the warped and unwrapped images. Clearly, over-blooming and low resolution are evident at the center of the warped image. After the image is unwrapped, the over-blooming and low resolution are concentrated in the top region. The red dashed line indicates a clearly imaged region. According to the optical simulation, this region corresponds to the fifth and sixth fields, which had smaller spot sizes than the other fields. Therefore, the RICE imaging system can improve image quality by processing because it can use the high-image-quality region for stitching.[7] The arrowhead points from the fifth field to the sixth field. Figure 7 shows some sequential images, both warped and unwrapped.

4.2 *Image Stitching*

After the images have been unwrapped, the images are stitched using MAE, MSE, and Pearson correlation coefficient–based methods. Figure 8 shows the image-stitching process. The reference and sample images are two serial images, which have overlapping regions and are shifted relative to each other by an angle that is determined by the rotation of the RICE. Therefore, the three algorithms can be used to compute the position of highest correlation; the sample image is shifted to this position, and then the clearly imaged region is reversed and stitched to the bottom of the reference image. This action yields a new combined image, which includes parts of the reference and sample images.

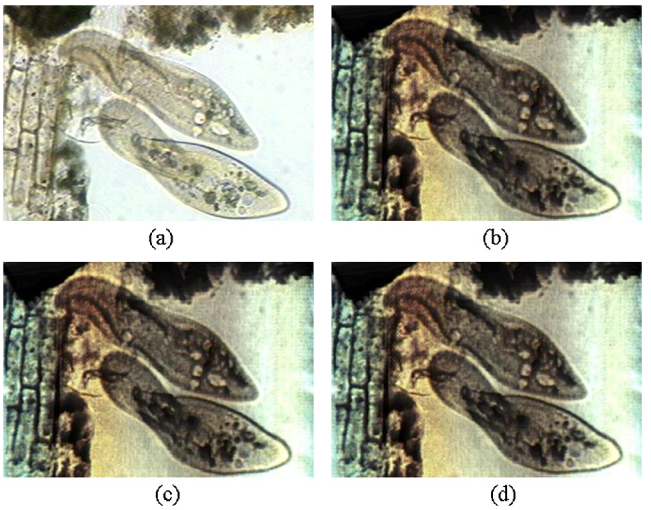

Fig. 9 (a) The simulated object sample, and image stitching after image processing by the (b) Pearson correlation coefficient, (c) MSE, and (d) MAE algorithms.

The computing resources used to process the images are an Intel Core 2 Quad CPU, a ASUS P5Q Q9500 motherboard, and 4 GB RAM. Figure 9 shows the object sample and the images that are reconstructed from the unwrapped images using the three algorithms. The three reconstructed images are very similar—they cannot be distinguished by the human eye. Their difference is determined using the peak signal-to-noise ratio (PSNR) formula, Eq. (6), in which the denominator MSE is as described above. The object sample and reconstructed image are used here, and the computation of PSNR transforms the colored image to the gray level to eliminate color distortion, which otherwise may affect the PSNR. Table 2 shows the results obtained using the three algorithms. The scan range is the block size of the sample image, which is used to scan the reference image so the position of highest correlation can be determined. The first four data in Table 2 were determined between two serial images. The results indicate that only the Pearson correlation coefficient algorithm is strong because the point of highest correlation does not vary with different scan ranges. However, the PSNRs of the MAE and MSE methods are lower than that of the Pearson correlation coefficient algorithm, which can be figured out from Eqs. (3) and (4). The two algorithms only consider the correlation of images by subtracting the image data directly. Unfortunately, if a singularity point (high intensity value) exists, it will affect the results when computing the correlation. The average computing time was about 6 sec because the Pearson correlation coefficient formula is more complex than MAE. Therefore, the following section uses only the Pearson correlation coefficient algorithm to reconstruct the images, which were captured in an experiment using a living animal.

$$\mathrm{PSNR} = 10 \times \log_{10}\left(\frac{255^2}{\mathrm{MSE}}\right). \tag{6}$$

4.3 *Experiment Using a Living Animal*

In the preceding section, an experimental environment that was ideal for image processing was established, enabling some otherwise problematic issues to be neglected. To model the practical use of RICE in the intestine, the ideal experiment should be replaced by an experiment using a living animal. The animal experiment involved a pig that had been raised in the white room of the Animal Technology Institute Taiwan. The pig was about two months old. Its belly was cut open by a professional surgeon to obtain the duodenum. Figure 10 shows the setup for the animal experiment.

The advantage of this animal experiment is that the RICE can move through the duodenum naturally because the living duodenum moves in a manner that pushes the RICE forward. Figure 11 shows the image reconstruction result of the duodenum by the Pearson correlation coefficient algorithm. It can be found that misalignment occurred because the best scan range is difficult to find, as the results of Table 2 indicate. The size of the scan range affects the image stitching results very seriously in the non-rigid world. Besides, the real intestine is not an ideal cylindrical shape, and the surface

Table 2 The image processing results of three algorithms.

	Data				
Algorithm	Scan range	Time (s)	Position	Value	PSNR
Pearson correlation cofficent	13×757	6.9	(217,1)	0.957	80.75
	12×757	6.5	(217,1)	0.957	80.74
	11×757	5.6	(217,1)	0.957	80.69
MAE	13×757	1.9	(217,1)	4.65	80.54
	12×757	1.8	(217,1)	4.65	80.52
	11×757	1.5	(218,1)	4.61	79.82
MSE	13×757	11.2	(217,1)	37.64	80.63
	12×757	10.8	(217,1)	37.37	80.50
	11×757	9.5	(218,1)	37.11	80.21

Fig. 10 The environment of the animal experiment.

is very rough. Hence, the optical transverse magnification is different in each field when RICE passes through the real intestine. Therefore, as mentioned previously, the image-stitching method should be improved in the non-rigid case. Figure 12 shows the deformation processing by using the vector comparison method. First, we used the Harris corner detector[21] to find the feature points of the two images S and T so that the feature points can form two vectors, each with a different intensity and direction. Therefore, the vectors should be tuned to the same intensity and direction. By computing the difference between the vectors, the gain of the x and y component between two images can be determined by Eq. (7),

$$\frac{V_{1x}}{V_{2x}} = G_x \qquad \frac{V_{1x}}{V_{2x}} = G_y, \tag{7}$$

where V_x and V_y are the lengths of the vectors in the x and y directions, respectively. Once the gain of the deformation points between two images is computed, it can be calibrated, which improves the misalignment problem. Figure 13 shows

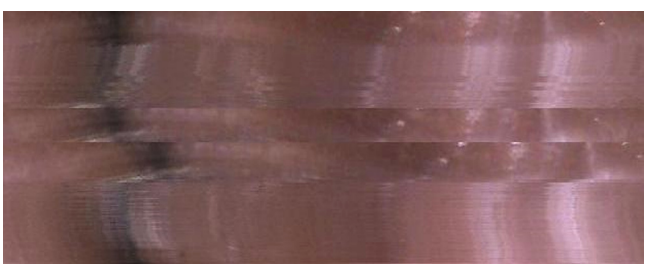

Fig. 11 The image stitching of a young swine duodenum by the Pearson correlation coefficient.

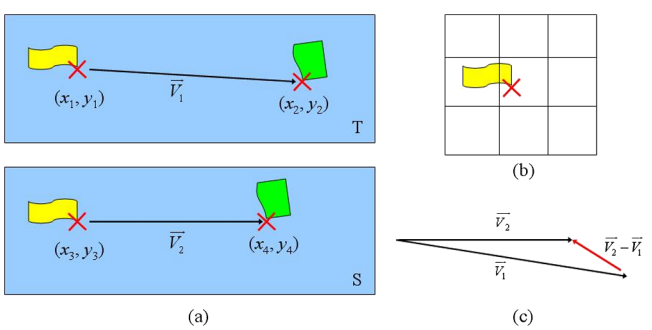

Fig. 12 Vector comparison method steps. (a) Using the Harris corner detector to find the matching points and connect the match points to form the vectors, (b) the corner is determined by a Harris corner detector block and (c) compared with the length and direction with the two vectors.

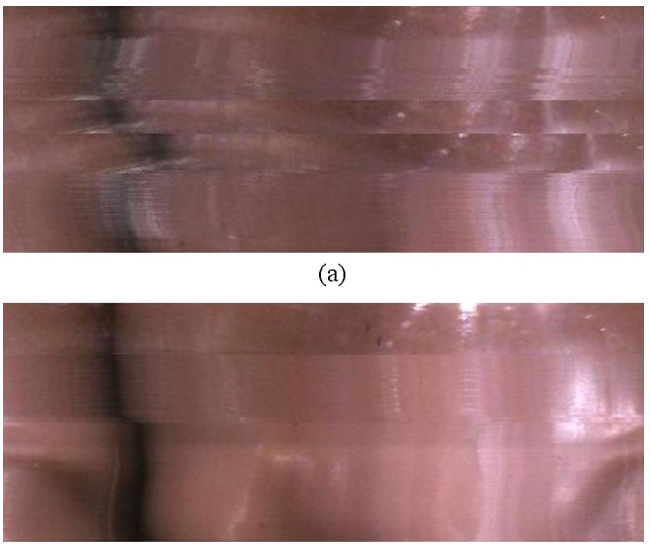

Fig. 13 The alternative methods of stitching images. (a) Pearson correlation coefficient; (b) vectors comparison method.

the stitching results between the Pearson correlation coefficient and vector comparison methods, and Fig. 14 shows the image stitching results (each result is stitched with 500 images). From the results, the misalignment problem can be improved by the vector comparison method and is better aligned than Pearson's method. However, Fig. 14(c) shows that some misalignment still occurred by using the vector comparison method. This is due to the RICE moving too fast in the intestine, which resulted in losing some image information and caused an unmatchable problem between two sequential images. This problem may be solved by increasing the camera frame rate. Another issue that should be dealt with is intensity inconsistency, which is due to light scattering by the liquid in the intestines, and produces the seam in the stitching result. This issue should be researched in more detail in the future.

4.4 *Image Reconstruction in Cartesian Coordinates*

This section discusses image reconstruction in the RICE system. Some fundamental concepts in geometrical optics are used to determine the geometrical positions. Figure 12 shows the positions of the object and the image, where point P_1 is the object point. To describe geometrical relations in RICE, Cartesian coordinates (r, θ, z) are used. Points v_1 and v_2 are imaged by the cone mirror at different times. Point I_1 and I_2 are the final images obtained by the lenses; S_O and S_I are the object and image distance; d is the air gap between the tip of the cone mirror and the object principal plane of the lenses; and R_O and R_I are the cone mirror radius of the object and image, where R_I also equals the image circle in the image plane. The terms H_1 and H_2 are the heights of I_1 and I_2, $z(t_1)$ and $z(t_2)$ are the heights of v_1 and v_1, M is the transverse magnification, and L is the distance between t_1 and t_2. The image plane in Fig. 15 shows the image point and R_I. The height and radius of the image plane can be determined from the given pixel size. Therefore, the transverse magnification M equals R_I/R_O, and S_I is about 2.86 mm.[7] Furthermore, the two similar triangles in Fig. 15 are used to get Eq. (8):

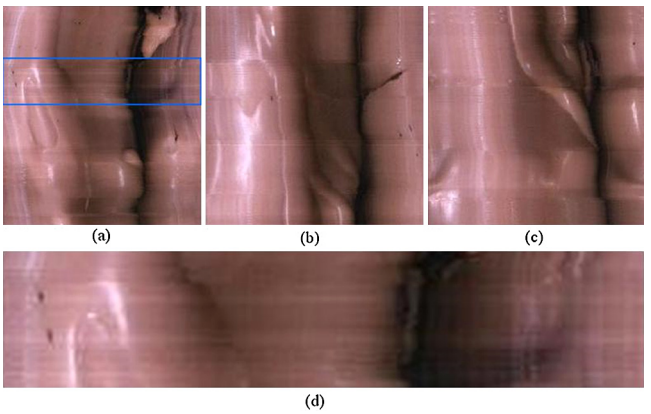

Fig. 14 The image stitch results with different patterns. Each pattern is stitched with 500 images. The images (a), (b), and (c) are stitched by using the vector comparison method. (d) The zoom-in view of the blue block in part (a); due to image information loss and intensity inconsistency, it does not look natural.

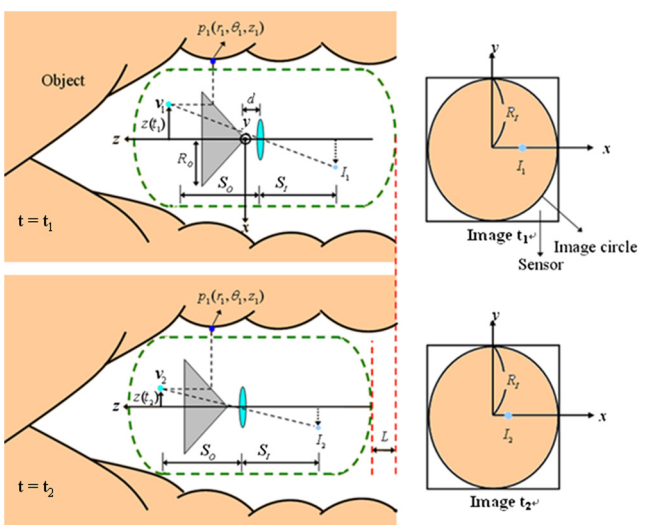

Fig. 15 The imaging relationship between two sequential images.

$$\frac{S_I}{r_1 + d} = \frac{H_1}{z(t_1)} = \frac{H_2}{z(t_2)} \tag{8}$$

where $z(t_1)$ equals z_1 because the angle between the cone mirror and the z axis is 45 deg, and $z(t_2)$ equals z_1-L. Rewriting Eq. (8) yields Eq. (9), which can be solved for the depth r_1 and position z_1 of the object.

$$\left.\begin{aligned} H_1 r_1 - S_I z_1 &= -H_1 d \\ H_2 r_1 - S_I z_1 &= S_I L - H_2 d \end{aligned}\right\} \Rightarrow r_1 = \frac{S_I L}{H_2 - H_1} - d, z_1 = \frac{H_1 L}{H_2 - H_1}. \tag{9}$$

That's the reason why RICE can use only one cone mirror and lenses to reconstruct the object. Figure 16 shows the image reconstruction of duodenum by Eqs. (8) and (9). The left side of this figure displays the full view of the stitching image with young swine duodenum, and the right side zooms in the rectangular range to show the depth information clearly.

Finally, the images captured by FICE and RICE should be compared. Figure 17 shows the intestine images captured by

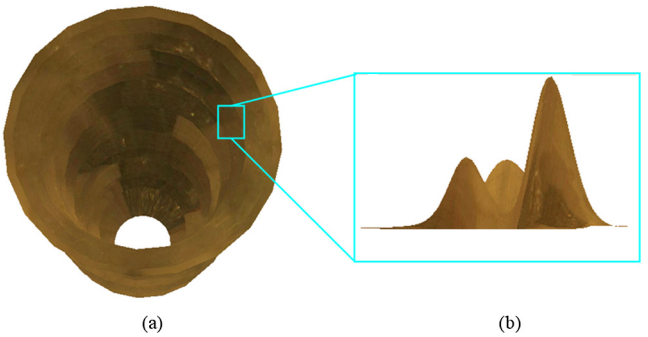

Fig. 16 Image reconstruction of duodenum (a) full view and (b) the zoom-in view of the block.

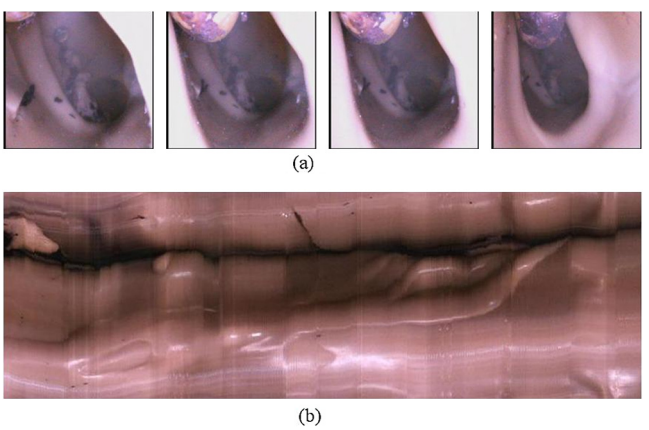

Fig. 17 The intestine images captured by (a) FICE and (b) RICE (after image stitching).

FICE and RICE. Figure 17(a) shows four images captured by FICE. Due to the depth of focus, the FICE can create clear images in a small area. On the other hand, the RICE takes the radial direction images, and the object distance is short. Hence, it doesn't need a long depth of focus, and after the clear parts of the images are selected to stitch, the image quality is better, as shown in Fig. 17.[7,22]

5 Discussion and Conclusions

In this work, images captured by the RICE system were processed and reconstructed using MATLAB software (MathWorks, Natick, MA). First, the image compression problem that is caused by the cone mirror is considered. It is solved by transforming the polar coordinates to rectangular coordinates. The second step is to identify a clear region in images to find the position of highest correlation between serial images, and then to stitch the images together. This work presented three algorithms for finding the position of highest correlation, involving the MAE, MSE, and Pearson correlation coefficient. An experiment under ideal conditions was carried out to compare these three methods. The method based on the Pearson correlation coefficient was the best: the position of highest correlation was independent of the scan range. The third step was to test the Pearson correlation coefficient-based method in a more complex case (in real intestines); thus, an experiment was carried out on a living animal. It was found that some misalignment occurred without any deformation processing. Hence, the vector comparison method was used to improve it. Finally, the image

was reconstructed using Eq. (9). All the object points were obtained using this equation, even when the RICE system had only one lens.

This work presents a preliminary image reconstruction algorithm. However, the reconstructed image that resulted includes some color distortion that is caused by color aberration, so future work must try to figure out how to compensate for this distortion by calibration. This calibration involves estimating the spectral sensitivity of the CCD sensor using eigen-spectrum methods. The estimated sensor spectral sensitivity can be mapped to real colors using the standard color mapping function of CIE 1931.

Acknowledgments

This work is supported by the National Science Council of Taiwan under contracts NSC 100-2220-E-009-033, 100-2218-E-039-001, and NSC 100-2623-E-009-006-D, and the "Aim for the Top University Plan" of National Chiao Tung University and the Ministry of Education, Taiwan. The authors would also like to thank the Chung-Shan Institute of Science and Technology, Delta Electronics Incorporation, and Dr. Jyh-Hung Lin of the Animal Technology Institute Taiwan, who provided experimental assistance and useful information. Finally, the authors are grateful to the instructor of technical writing, Ted Knoy, who helped them edit the manuscript for grammatical and stylistic writing errors.

References

1. Given imaging, "M2A given diagnostic system," http://www.givenimaging.com/.
2. G. D. Meron, "The development of the swallowable video capsule (M2A)," *J. Gastrointest. Endosc.* **52**(6), 817–819 (2000).
3. C. Gheorghe, R. Iacob, and I. Bancila, "Olympus capsule endoscopy for small bowel examination," *J. Gastrointest. Liver Dis.* **16**(3), 309–313 (2007).
4. A. Uehara and K. Hoshina, "Capsule endoscope NORIKA system," *Minim. Invasive Ther. Allied Tech.* **12**(5), 227–234 (2003).
5. T. Nakamura and A. Teran, "Capsule endoscopy: past, present, and future," *J. Gastroenterol.* **43**(2), 93–99 (2008).
6. T. Kav and Y. Bayraktar, "Five years' experience with capsule endoscopy in a single center," *World J. Gastroenterol.* **15**(16), 1934–1942 (2009).
7. M. Ou-Yang and W. D. Jeng, "Design and analysis of radial imaging capsule endoscope (RICE) system," *Opt. Express* **19**(5), 4369–4383 (2011).
8. V. N. Mahajan, "Optical imaging and aberrations, part i: ray geometrical optics," Chapter 1, in *Gaussian Optics*, SPIE Press, Bellingham, WA p. 7 (1998).
9. L. Spacek, "A catadioptric sensor with multiple viewpoints," *J. Robot. Autom. Syst.* **51**(1), 3–15 (2005).
10. W. D. Jeng et al., "Design of illumination system in ring field capsule endoscope," *Proc. SPIE* **7893**, 78930E (2011).
11. L. Yao and M. Lizhuang, "A fast and robust image stitching algorithm," in *Proc. of 6th World Congress on Intelligent Control and Automation*, Dalian, China, pp. 9604–9608 (2006).
12. X. Fang et al., "New multi-resolution image stitching with local and global alignment," *J. IET Comp. Vis.* **4**(4), 231–246 (2010).
13. Q. Zhu and K. Li, "Image stitching using simplified SIFT," in *Proc. of Information and Automation, IEEE International Conference*, Harbin, pp. 1134–1137 (2010).
14. T. Yu and J. Huiyan, "Highly efficient image stitching based on energy map," *Proc. of the 2009 2nd International Congress on Image and Signal Processing*, Tianjin, China, pp. 1–5 (2009).
15. S. K. Bar-Lev, B. Boukai, and P. Enis, "On the mean squared error, the mean absolute error and the like," *Comm. Stat.—Theory Methods* **28**(8), 1813–1822 (1999).
16. D. M. Allen, "Mean square error of prediction as a criterion for selecting variables," *Technometrics* **13**(3), 469–475 (1971).
17. C. J. Willmott and K. Matsuura, "Advantages of the mean absolute error (MAE) over the root mean square error (RMSE) in assessing average model performance," *Clim. Res.* **30**(1), 79–82 (2005).
18. H. C. Huang and Y. P. Hung, "Adaptive early jump-out technique for fast motion estimation in video coding," *J. Graph. Mod. Image Proc.* **59**(6), 388–394 (1997).
19. L. Egghe and L. Leydesdorff, "The relation between Pearson's correlation coefficient r and Salton's cosine measure," *J. Am. Soc. Inform. Sci. Tech.* **60**(5), 1027–1036 (2009).
20. Y. Wang and L. P. Xu, "A global optimized registration algorithm for image stitching," in *Proc. of 1st International Congress on Image and Signal Processing*, Sanya, China, pp. 525–529 (2008).
21. C. Harris and M. J. Stephens, "A combined corner and edge detector," *Proc. Alvey Vision Conf.* 147–152 (1988).
22. M. Ou-Yang et al., "Optimizing the depth of field for short object distance of capsule endoscope," *Proc. SPIE* **6859**, 68591Q (2008).

Mang Ou-Yang received a BS degree in control engineering in 1991, and MS and PhD degrees in electro-optical engineering, in 1993 and 1998, from National Chiao Tung University, Hsinchu, Taiwan. He worked for the Precision Instrument Development Center, National Science Council of Taiwan, and was in charge of optical metrology for space application from 1994 to 2000. Thereafter, he worked for Klaser Technology Co. as the leader of the R&D group for developing projection display technology. Since 2004, he has been at the Institute of Optical Sciences, National Central University, Jhongli, Taiwan, as an assistant professor. His research interests are related to optoelectronics industrial instrumentation development, including biomedical optics, microthermal sensors, readout electronics, and projection display technology.

Wei-De Jeng was born in Taiwan in 1986. He received a BS degree from the Department of Electrical Engineering from National Taiwan Ocean University, Taiwan, in 2008 and an MS degree in the Department of Optics and Photonics Engineering from National Central University, Taiwan, in 2010. He is currently studying toward a PhD in the Department of Electrical and Control Engineering at the National Chiao-Tung University. His research interest is the biomedical field.

Yin-Yi Wu received an MS degree in electronic and information from the National Yunlin University of Science and Technology, Taiwan, in 1999, and is currently pursuing a PhD degree in electrical engineering at National Chiao Tung University, Hsinchu, Taiwan. He joined the Materials and Electro-Optics Division at the Chung-Shan Institute of Science and Technology. His current interests include integrated-circuit design and image processing.

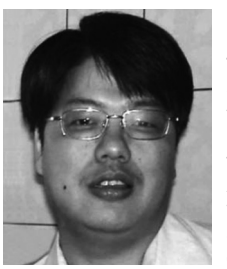

Lan-Rong Dung (SM'93–M'97) received a BSEE degree from Feng Chia University, Taiwan, in 1988; an MS degree in electronics engineering from National Chiao Tung University, Hsinchu, Taiwan, in 1990; and a PhD in electrical and computer engineering from the Georgia Institute of Technology, Atlanta, in 1997. From 1997 to 1999, he was with Rockwell Science Center, Thousand Oaks, CA, as a member of the technical staff. He joined the faculty of National Chiao Tung University, Taiwan, in 1999, where he is currently an associate professor in the Department of Electrical and Control Engineering. His current research interests include very large scale integrated design, digital signal processing, hardware-software codesign, and system-on-chip architecture. Professor Dung received the Best Student Award from Feng Chia University, Taiwan, in 1988. He received the VHDL International Outstanding Dissertation Award Celebration in Washington, D.C., in 1997. He is a member of the IEEE Circuits and Systems and Signal Processing societies.

Hsien-Ming Wu was born in Taiwan in 1946. He received his MS degree in chemistry in 1971 and a PhD in chemical engineering from Tsing-Hua University in 1986 in Taiwan. From 1995 to 2001, his major research focus was on the conductive polymer, OLED and MEMS. Until 2005, his research focused on bio-medical instruments, especially the capsule endoscope and digital X-ray, DR, and CR sensor.

Ping-Kuo Weng earned his BS degree in nuclear engineering from the National Tsing Hua University of Taiwan in 1985. In 1992, he received his PhD degree at the Institute of Electro-Optical Engineering, National Chiao Tung University. Since then, he has been working at the Chung-Shan Institute of Science and Technology in the Solid-State Devices Section. His current research interests include CMOS image sensor design, cameras for medical imaging systems, and system-on-chip architecture.

Ker-Jer Huang was born in Taiwan in 1964. He received a BS degree from the Department of Power Mechanical Engineering from National Tsing-Hua University, Taiwan, in 1986, and an MS degree at the Institute of Aeronautics and Astronautics Engineering of National Cheng-Kung University, Taiwan, in 1988. He is currently working toward a PhD at the National Tsing Hua University. His research interest focuses on the microfluidic and biomedical fields.

Luan-Jiau Chiu was born in Taiwan in 1960. She received a BS degree at the Department of Computer Science from Feng-Chia University, Taiwan, in 1982, and an MS degree in the Department of Electrical Engineering and Computer Science from Yuan-Ze University, Taiwan, in 1998. She worked as a research assistant at the Chung-Shan Institute of Science and Technology beginning in 1984. In 1998, she became an assistant research fellow in medical region. Her research interest focuses on image processing, especially in the biomedical field.